ISSN 1063-7710, Acoustical Physics, 2010, Vol. 56, No. 6, pp. 951–961. © Pleiades Publishing, Ltd., 2010.

Methods of Measuring Characteristics of Oscillations and Waves in Micromechanics (A Review)

I. V. Simonov

Institute for Problems of Mechanics, Russian Academy of Sciences, pr. Vernadskogo 101-1, Moscow, 119526 Russia
e-mail: simonov@impnet.ru

Received March 2, 2010

Abstract—Methods of recording the electric signals generated during wave oscillations and wave propagation and the results of experiments on determination of dynamic characteristics of thin fibers and films are reviewed. New experimental setups have been developed. A possibility of studying the spectra of fiber oscillations is demonstrated, and a method for determining nonlinear stress-strain diagrams based on variations in the frequencies of transverse oscillations of this fibers as strings is proposed. The effect of sharp deceleration of dispersal of a charge being coated on the specimen surface in case of a damaged glass fiber is discovered. A complex method for measuring wave and mass velocities of elastic waves and instant elasticity moduli of a fiber during simultaneous high-speed photography and recording of electromagnetic radiation is developed. The dependences of these quantities on the wave intensity are given, and the scale effect is revealed. Application of this method for studying wave processes in thin polymer films is demonstrated.

DOI: 10.1134/S1063771010060205

INTRODUCTION

One of the most important problems of mechanics is construction of the models of behavior of materials and structure elements. The problem of model construction, namely, the determination of material parameters and functions entering constitutive equations, is often solved experimentally. The viscoelastic properties of polymer fibers and films have been extensively studied in the literature [1–3]. The method of free torsional oscillations, the method of forced resonant flexural oscillations, and the method of buffer rods for measuring velocities of longitudinal and shear waves are the most widely used and promising for studying propagation of acoustic waves in such bodies [2]. A substantial dependence of the acoustic wave velocities on the frequency, temperature and structure of a polymer has been revealed. However, experimental studies on the propagation of finite-amplitude waves in a thin specimen are unknown. At the same time, the study of dynamic processes in micromechanics, namely, in fibers and films with one or two characteristic dimensions in a micron range, is evidently of certain scientific and practical interest. Thus, composite materials reinforced by fiber beams or thin layers are used in devices designed for protection from a shock or an explosion for the maximal absorption of the kinetic energy of a striker or shock waves. Cables and ropes are subjected to shock loads in many situations: during airplane landing on the deck of an aircraft carrier, in mountaineering, etc. The problem of optimization necessitates performing experiments on calibration of the models of behavior of micron-size bodies during wave loads. Application of traditional methods is either impossible owing to the reasons related to smallness of the transverse dimensions of the tested specimens or rather complicated.

The proposed methods of studying finite-amplitude waves is based on self-generation of an electric signal by a dynamic process. From the physical point of view, this phenomenon is explained by a relative motion of charges at an atomic-molecular level that, in accordance with the laws of electrodynamics, generated an alternating electric field in the ambient space. Recording of this field gives data on the mechanical processes that take place in this case. Generation of the electromotive force during rupture or shock compression of different substances has been studied in many works. It was revealed [4] that a field can be recorded not only from a shock wave, but also during any dynamic deformation of the medium, if the equipment is sensitive enough. Possibilities of using electrets as sensors of displacements and deformations are considered in monograph [5].

All known works on recording of electromagnetic radiation (EMR) from dynamic processes considered bodies with macrodimensions. The question arises of whether a stable recording of an electric signal from these processes is possible in fine structural elements. With this aim in view, unique, highly sensitive experimental setups for recording electric signals during oscillations and propagation of longitudinal waves in fibers and films have been developed.

The review given below includes a study of fiber oscillations using the method of electric signal record-

ing and determination of the stress-strain curves of fiber by measuring the frequency of the first shape of transverse oscillations depending on deformation; application of the EMR-effect for determining the velocity of a longitudinal elastic wave in polymer fibers of different diameters and, as a result, the elasticity modulus as functions of the wave intensity; and presentation of a complex method of measuring wave and mass velocities in fibers and films during simultaneous recording of EMR and high-speed photographing.

RECORDING OF OSCILLATIONS AND MEASUREMENT OF FIBER CHARACTERISTICS

Experimental investigations of fine fiber oscillation gives information on the rheological parameters of microobjects. Since, contrary to nonstationary wave processes, the deformation gradients and, consequently, the generated EMR during oscillations are negligible, an electric charge is preapplied onto the surface of a tested object. The frequencies are measured by recording variations in the inductive component of the electric field from these mobile charges during transverse oscillations of the fiber with an antenna sensor.

The main elements of the experimental setup developed for studying oscillations and recording electric signals from the macrosize bodies are the electric field sensor (an antenna) and loading and recording devices. The loading device, namely a cross-arm, has two metal clamps for fixing a fiber, one of which is fixed and the other of which can move horizontally with the help of a rod. To screen the sensor and the clamps from the external magnetic field, they are placed in a box from a brass frame with the dimensions $162 \times 89 \times 32$ mm and walls 7 mm thick; the box is covered by the upper and the lower aluminum covers 1 mm thick. The sensor was connected to a recording device either via a source follower characterized by a very high input resistance on the order of 100 Ohm or via oscillographic testers with an active resistance of 10^6 Ohm and an input capacitance of 15–35 pF. It provided for a possibility to change the input resistance and the input capacitance for recording the processes with the duration from several seconds (static processes of charge dispersal on the fibers) or a fraction of a microsecond (dynamic processes). A LeCroy Wave Surfer 422 dual-beam digital oscilloscope with a frequency band of 200 MHz limited by 20 MHz to reduce substantial high-frequency losses was used as a recording device. A source follower designed based on the unipolar FET KP305D was on a separate screen fixed to the external screen of the setup. The frequency band of the source follower with a RK50 cable 0.8 m long was limited by 10 MHz. A flat electric field sensor 7×6 mm in size consisting of thin parallel conducting stripes served as an electric field sensor. It has a dielectric coating and was fixed on a glass plate $18 \times 11 \times 2.5$ mm in size which, in its turn, was glued on anther glass plate $49 \times 15 \times 2.5$ mm in size fixed to the lower cover of the external screen. A copper wire rod 2 mm in diameter and 10 mm long was also used as antenna. Both were sensors of capacitance type, and their self-capacitance was 1–2 pF for the rod and 30–60 pF for the flat sensor (the higher the sensor capacitance, the higher its sensitivity, but the signals even from the rod sensor were recorded without amplifiers). The specimens were fixed in the clamps between dielectric layers above the sensor few millimeters away from it. The oscilloscope was started by the forefront of the recorded signals. The results of testing and adjustment of the technique are given in detail in [6].

Determination of the Tension Curve Based on Frequency Measurements

An experiment with excitation of transverse oscillations of charged polymer fibers extended up to 2–15% deformation (Japan fishing line manufactured by Nikko Vexter; diameters $d = 60$, 80, and 100 μm; length $L_0 \approx 2$ cm) as strings showed as follows [7]:

1. Fiber oscillations are not recorded without charge application;

2. If a negative (positive) charge is preliminarily applied with the help of an ebonite (glass) stick electrified by rubbing against wool (silk), then the initial phase of the signal during initial displacement of the fiber center in the direction from the sensor is positive (negative).

3. The period of oscillations by the first shape T_1 and the damping coefficient, as well as the period of the oscillation plane rotation in the case in which this effect appears, can be determined with good accuracy based on the oscillograms (see the example in Fig. 1). The effect of the charge value and sign on T_1 was not revealed. Due to nonsymmetric excitation a superposition of the oscillations by the next shapes is observed and frequencies are determined.

Let us transform a classical formula for the first frequency of the string characteristic oscillations:

$$f = \frac{1}{2L}\sqrt{\frac{F}{m/L}} = \frac{1}{2L_0}\sqrt{\frac{\sigma}{\rho(1+e)}},$$
$$e = \frac{L - L_0}{L_0}, \quad \sigma = \frac{F}{S_0}, \tag{1}$$

where F is the tensile force and m, L_0, L, ρ, and S_0 are the mass, initial and variable lengths, and initial density and area of the string, respectively. From Eq. (1) there follows a relationship between the normal stress σ and the frequency f,

$$\sigma = 4f^2L_0^2\rho(1+e). \tag{2}$$

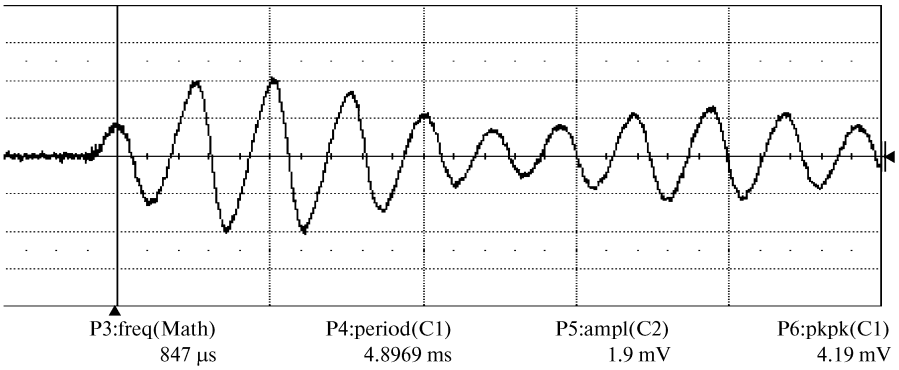

Fig. 1. A typical oscillogram of fiber oscillations with rotation of the oscillation plane.

By measuring the dependence of the frequency of characteristic oscillations of a stretched fiber on its deformation $f = f(e)$ and substituting it in Eq. (2), we obtain the stress-strain curve $\sigma = \sigma(e)$ [8].

The experiments on transverse oscillations of a fiber from a silica glass, type VMP, as an elastic cantilever with the length $L_0 = 18, 30$ mm (with the diameter $d = 150$ μm, density 2.58 g/cm^3, and the elasticity modulus of 70–95 GPa based on different data) have also been performed. The oscillations were excited by an impact on a clamp. The conclusions were the same as those made in the experiments with a polymer fiber. For example, the experiments showed that the period of oscillations $T_1 = 3.7, 4.8$ μs within the measurement accuracy (two signs) does not depend on the value and the sign of the induced charge and, in addition, on the damage acquired during oscillations. According to the theory of oscillations of an elastic cantilever, the elasticity modulus during bending is then determined by the formula $E_f = \rho_0 L_0^4 (0.14 d T_1)^{-2}$. The calculations give $E_f = 44,39$ GPa. These values are substantially smaller than the data for the elasticity modulus obtained in the experiments on the fiber long-term tension. The fact that the elasticity modulus depends on the experimental conditions (extension, bending, etc.) is well-known from the literature.

The Effect of the Velocity Dependence of the Charge Flow from the Surface of a Glass Fiber on the Level of Its Damage

This effect was revealed in experiments on multiple excitation of oscillations. The time intervals between the cycles were on the order of a second, which is much larger than the time of complete damping of one oscillation cycle (about 250 ms) at the number of oscillations in a cycle on the order of 50. The results were unexpected. Based on the pattern of damping of the maximal signal amplitude in a cycle, we observe the time evolution of the electron flow-off up to zero (see Fig. 2). Assuming the charge value to be proportional to the signal amplitude, it can be calculated that a tenfold decrease of the charge occurs for 4 s and there are six excitation acts during this period. This evolution cannot be revealed in experiments with a positive charge, since the charge flows off the fiber practically instantly and the repeated oscillation does not yield signal generation.

After several runs of such experiments, the tested fiber acquires damage in the form of surface microcracks and holds a negative charge for a long time. It follows from the oscillogram in Fig. 3 that the time required now for a tenfold charge decrease is 40 s and the number of excitation acts during this period became 50, i.e. the values changed by one order. The photos in Fig. 4 showing glass fiber specimens without flaws before the tests (two specimens to the right) and those with flaws after the tests (three specimens to the left) with an 80-fold magnification serve as a verification. Note that the air humidity during these experiments is a substantial parameter.

The following experiment is of interest. Let us apply a negative charge on the damaged fiber and observe the signals characteristic for this charge and then apply a positive charge and observe different signals. Continuing to excite oscillations during short intervals, we can be persuaded that the charge on the fiber changes its sign with the change of the initial signal phase. The explanation of this and the previously described effects is as follows: microcracks hold electrons much better than ions with larger masses and sizes.

Wetting of the solid surface with an "electron fluid" is similar to the phenomenon of wetting with a fluid used in the method of capillary flaw detection. It may become a basis for developing a new method of nondestructive testing of the surfaces of bodies with micron and, probably, nanosizes.

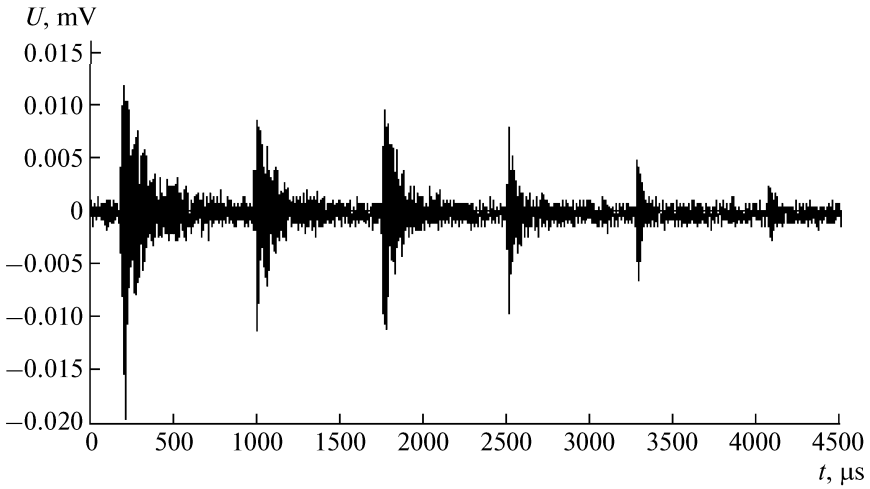

Fig. 2. A relatively fast flow-down of electrons from an undamaged glass fiber.

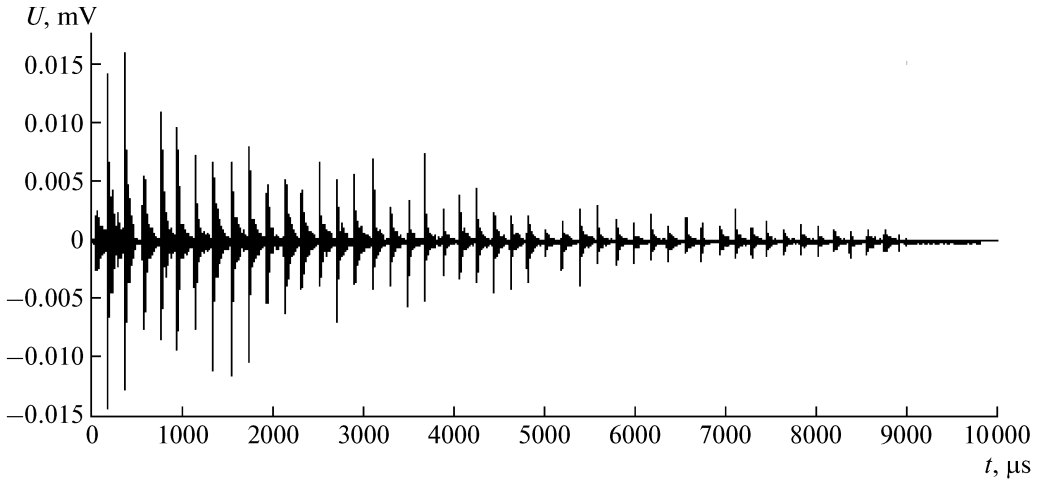

Fig. 3. A relatively slow charge flow-down from a damaged fiber.

METHODS OF MEASURING WAVE AND MASS VELOCITIES

The main elements of the setup for measuring wave velocities are a LeCroy Wave Surfer 422 dual-beam digital oscilloscope, the sensors of the electric field (antenna), and a cross-arm for fixing and rigid loading of a specimen, which allows varying its length within the range of 1–70 cm. The cross-arm has two metal clamps, one of which is fixed and the other of which can move horizontally with the help of a rod. The clamps and the entire experimental setup are grounded.

The scheme of the experiment is shown in Fig. 5. After many tests two sensors were mainly used for EMR recording, namely, two- and three-turn spirals made of an insulated copper wire. The inner diameter of the turn in the experiments with fibers is <1 mm; in the experiments with narrow film stripes, the turn had a form of a narrow oval. The sensors are connected with the channels C1 and C2 of the oscilloscope. The specimen with the length L_0 was passed through sensors positioned at the distance l (a base) from one another and was fixed in the clamps. The fiber was extended by the length ΔL providing for the specified deformations $e = \Delta L/L$ and was kept in such a state to relax the stresses (as a rule, not longer that 1 min; some experiments were performed with the aim to determine stress relaxation), and the narrow film stripe was fixed with a slight extension. Then a cut was made along the normal to the specimen surface with a razor blade at the distance l_0 from the nearest sensor to the depth h. The value of h for a film stripe was specified, whereas that for a fiber was critical: when it was reached, the tensile load became limit and broke away the specimen and an unloading wave started propagating from the formed free edge. The force transmitted via a movable rod was applied by a jerk to the end of the

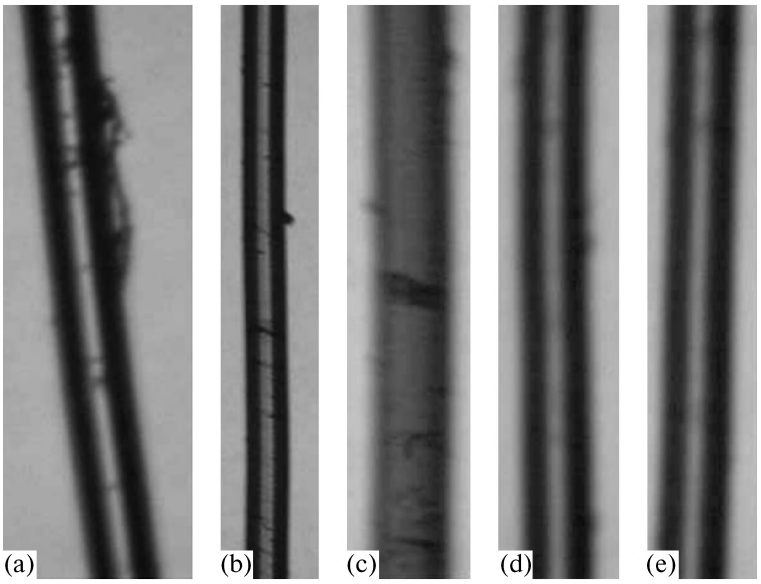

Fig. 4. The presence (a, b, c) and absence (d, e) of microdamage on the surface of a glass fiber.

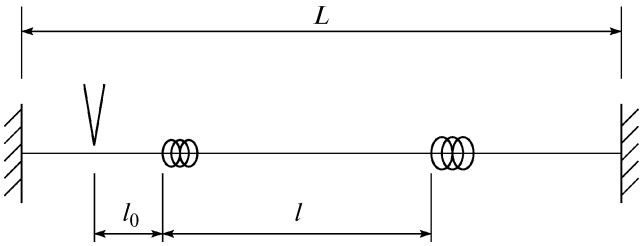

Fig. 5. Positioning of sensors C1 (right) and C2 (left) during wave velocity measurements.

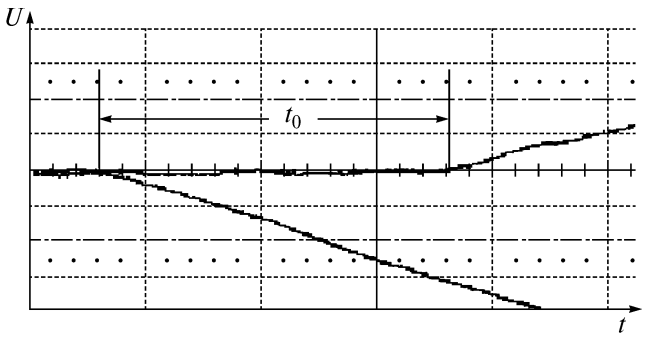

Fig. 6. Typical oscillograms of signals. Time base—10 μs/div, voltage base U—10 mV/div.

film stripe for its rupture and for the unloading wave generation. Fast processes of fracture and wave formation yielded variations in the electric field in the vicinity of the specimen in the radio-frequency range. This is the nearest region where field variations are quasistatic rather than wave ones. However, as applied to mechanical processes, they are termed in the literature as electromagnetic radiation. The antennas are connected to similar electric circuits of the oscilloscope and, thus, EMR of a sufficient intensity yields formation of two oscillograms on the oscilloscope screen, namely, electric tension–time dependences: $U = U(t)$. They are used to determine the signal diversity t_0. In the case of fine fibers, it is the difference of the time of the signal beginning (see Fig. 6); the method of determining t_0 for a film is shown below. Then the wave velocity was calculated based on the formula $c = l/t_0$.

Determination of the Dependence of the Unloading Wave Velocity in Polymer Fibers on Its Intensity. A Scale Effect

The experiments were performed using fibers made of a copolymer of the type Nikko Vexter (NV) with diameters 60, 100, and 140 μm and nylon fibers of the type Broad Nylon Monofilament (BNM) with diameters 60, 120, and 180 μm (Japan). Depending on the loading rate and their diameter the fibers can withstand the deformations until damage of about 15% (NV) and 40% (BNM). With the aim of performing a comparison, the stress-strain curves $\sigma = \sigma(e)$ in the case of slow loading and unloading from the given loading state were preliminary determined. By differentiating the equations of the trend lines of the experimental points during unloading, the long-tern elasticity moduli E_∞ corresponding to the origin of the curves of elastic unloading from the states with the specified deformations e were determined. Table 1

Table 1. Long-term elasticity moduli during unloading from a specified loading state

e, %	2	3	4	5	7	10
E_∞, GPa	2.94	3.23	3.75	4.39	7.03	25.28

Table 2

	NV			BNM		
d, mm	0.14	0.1	0.06	0.06	0.12	0.18
A, km/s	2.24	2.11	2.47	1.29	0.902	0.902
B, km/s	0.143	0.225	0.242	0.12	0.112	0.116

exemplifies the dependence $E_\infty(e)$ for the NV fiber ($d = 60$ μm).

Theoretical Aspect

The rheology of fibers from a copolymer and nylon is nonlinear hereditary viscous elasticity, but a linear elasticity theory with instant elasticity moduli E may be used to describe fast processes at relatively small deformations in the unloading wave (despite the fact the extension was carried out for large deformations) [9]. Generally speaking, owing to nonsymmetry of unloading, a complex wave spectrum (of the type of Pohgammer–Crie waves) starts propagating from the fiber free end after a quasistatic process of a cut at a critical depth depending on tension and a nearly instant break of a fiber. However, it follows from the elementary physical considerations that the stored elastic energy is mainly transformed to the energy of the zero mode, i.e., to the energy of an elementary dispersionless longitudinal wave in an elastic thin rod propagating with the constant velocity c (it being verified by independent experiments).

Thus, the wave processes in a fiber can be interpreted based on the hypothesis of a thin semi-infinite rod where an elastic steplike unloading wave propagates. Minor variations in the density ρ in the performed experiments allow considering it equal to the initial density of 1140 kg/m^3 (NV) and 1163 kg/m^3 (BNM). The velocity c determined using the base l and signal diversity t_0 and the modulus E depend on preliminary (large) deformation of the fiber e. However, deformation variations at the wave fronts during unloading turned out to be very low (then being followed by a slow process of creep with partial or complete regeneration of the specimen) and use of the linear elasticity theory is justified in this case if we assume that there is at least a substantial sector of unloading close to a linear one. As it will be revealed later, the lower the initial deformation e, the more accurate the linear approximation.

According to the law of conservation of momentum, let us express the stress jump at the wave front σ and a corresponding elasticity modulus E through the front velocity c and a jump of the mass velocity v using the known formula

$$\sigma = \rho c v = \rho \Delta e c^2, \quad \Delta e = e - e_*, \quad E = \rho c^2, \quad (3)$$

where $e_* = e_*(e)$ is the instant residual deformation beyond the unloading wave front.

Now let us substantiate that the measured velocity and a corresponding elasticity modulus are really instant. In the linear theory of the hereditary-elastic medium, the approximate description of waves in a rod is similar to the description of waves in an elastic medium: the shear deformation and transverse inertia are neglected, and the main difference in the wave equations is related to the fact that elastic constants are substituted by the operators. An asymptotic analysis of the solution of the problem of the load instantly applied to the rod end and then remaining constant gives the following pattern of the wave front propagation [9]. At first ($t \to 0$) it moves with a instant velocity corresponding to the modulus E. The asymptotic at $t \to \infty$ gives a long-term front velocity $c_\infty = \sqrt{E_\infty/\rho}$. Since several-fold variations in the base length did not demonstrate a substantial difference in the velocities c, which are substantially higher than c_∞, these velocities were interpreted as instant.

The signs in Figs. 7 and 8 show the experimental velocities of the longitudinal waves in NV and BNM fibers of different diameter averaged over 10–15 tests. They are approximated by the linear dependence

$$c = A + Be. \quad (4)$$

The values of the constants A and B are listed in Table 2. Substitution of $c = c(E)$ from Eq. (4) to Eq. (3) yields a quadratic dependence of the modulus E on the deformation e. The instant elasticity moduli exceed their prolonged values listed in Table 1 by 20–50%, which points to the degree of the viscosity effect. The scale effect lies in the dependence of the velocity c and the instant elasticity modulus at the fixed deformation e on the fiber diameter: the higher the velocities $c = c(e)$, the smaller the fiber diameter (the fibers become harder), although from the point of view of macroscopic continuum mechanics they are to coincide. Thus, at $e = 10\%$ the difference between the velocities at $d = 60$ and 140 μm is about 1 km/s. It is interesting to note that the scale effect disappeared for the BNM fiber when turning to thicker fibers (see Fig. 8). The dependences $E = E(d^2)$ on the diameter square, i.e., on the cross section area, at a fixed deformation turned out to be close to linear ones. It is clear that the investigations of the scale effect with respect to the tested fiber materials are not complete, since there were no specimens with smaller diameters. However, let us remember that the main aim of the problem is to develop a new method and demonstrate that this

method can be used to obtain data on the dynamic properties of micron-size bodies.

Based on the dependences shown in Figs. 7 and 8, it is possible to estimate variations in the elastic deformation from e to e_* in the unloading wave with the formula $e - e_* = 100\%\sigma/E$. Thus, for the deformations $e = 12$ and 14% reached at $d = 100$ and 140 μm, we find that $E \approx 28$ and 22 GPa, $\sigma \approx 0.5$ and 0.68 GPa, and $e - e_* \approx 1.8$ and 3%. Thus, in the case of the maximum value of fiber deformations, the unloading deformation was only 15–20% from the initial value of e (let us say again that the residual deformation in the fiber e_* then decreases owing to creep). For a small initial deformation $e = 2\%$, the estimate gives $e - e_* \approx 0.63\%$ for these two diameters, i.e., a relative deformation jump on the front of the unloading wave is larger: $(e - e_*)/e \approx 30\%$. These data also qualitatively point to the degree of the effect of fiber material viscosity during dynamic unloading from different initial states.

Sometimes the measurements along the base of the difference of the times of arrival of longitudinal wave yield large or small values. Often it is difficult to determine the time t_0 based on oscillograms. These irregularities are explained by the asymmetry of rupture and a complex structure of the fiber material. Polymers consist of the clusters of long molecule beams with weak bonds (Van der Waals ones), whereas the bonds in long molecules are strong covalent ones (polymer stochastic bonds are simulated by random fractals). In addition, a discrete size distribution of flaws in the volume (predominantly of microcracks) is fixed [1]. The propagation of the stress wave over such a structure is a complex process if we consider it at the molecular level, and this is reflected in the recorded signals: only some oscillograms obtained during N identical experiments have a shape ideal for measuring t_0, it being shown in Fig. 6 (the variability of shapes of the curves $U = U(t)$ was discussed in [6]). Since in $N_1 < N$ experiments ($N_1/N \approx 0.2$–0.4) determination of the wave velocity was complicated and they were not used in statistics, the corresponding fiber specimens belonged to imperfect ones: they seem to contain anomalous flaws (or an abnormally large number of "usual" flaws) distorting the result. Different authors pointed to such a possibility [1, 3]. Moreover, there always may be situations in which rupture yields generation of the dispersion modes significant for the equipment sensitivity the velocities of which, judging by the solutions to the known Pohgammer–Crie problem, are much higher than the velocity of the zero mode.

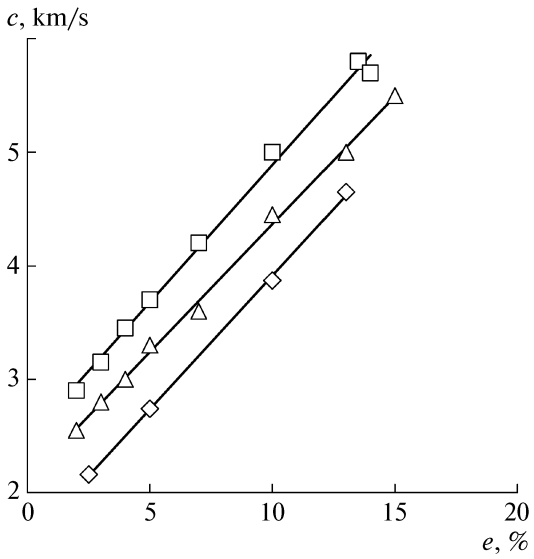

Fig. 7. The velocity of the longitudinal unloading wave in NV fiber as a function of initial deformation: (□) $d = 60$, (△) $d = 100$, and (◇) $d = 140$ μm.

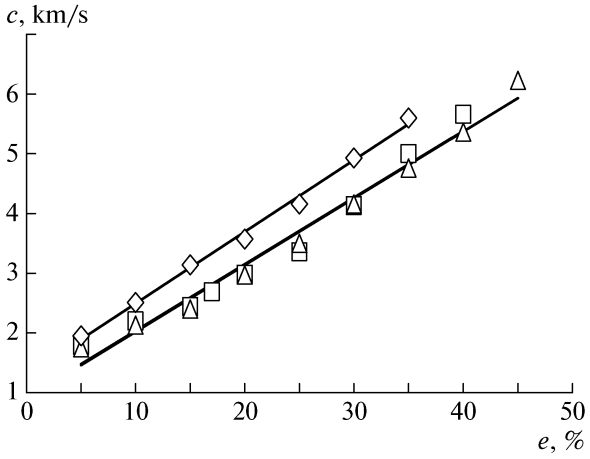

Fig. 8. The velocity of the longitudinal unloading wave in BNM fiber as a function of initial deformation: (□) $d = 60$, (△) $d = 120$, and (◇) $d = 180$ μm.

A Complex Method of EMR Recording and High-Speed Photography for Measuring Wave and Mass Velocities in Polymer Fibers and Films

A complex technique for determining characteristics of wave processes in polymer fibers and films using recording of electromagnetic radiation and high-speed photography with a video camera has been developed. A fiber was rigidly fixed in clamps at a specified extension and kept there for some time for the stress relaxation to take place and to start considering that the initial state is on the curve of long-term loading $\sigma = \sigma(e)$ of the fiber obtained during independent measurements. Then the fiber was slightly cut by a sharp razor and at some moment it began rapidly rup-

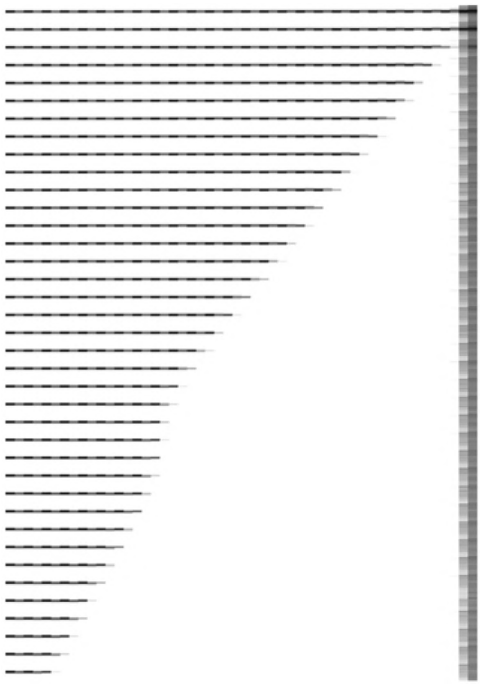

Fig. 9. Video filming of the fiber end displacements: d = 280 μm, e = 5%, L_0 = 231 mm.

ture at the place of the cut under the action of the stretching force. The velocity of the longitudinal unloading wave was determined using the EMR method described above. Video filming with the velocity 45000, 73000, or 109000 frames per second performed using powerful light sources makes it possible to measure the mass velocity beyond the wave front and its variations after the reflected wave based on the motion of a fiber end formed after rupture (see Fig. 9). Then different scenarios of instability development can be observed: initiation, growth, and propagation of transverse waves after wave reflection at the place of fixation in the form of a compression wave. Lengths, amplitudes, and velocities of the waves, as well as instant elasticity moduli corresponding to unloading from the stretched state and bending, are determined [11, 12].

Let us demonstrate the determination of the mass velocity using the example of NV fiber testing under the following initial conditions: d = 300 μm, L_0 = 46 mm, e = 10%, σ = 198 MPa, Δt = 13.7 μs (the interval between the filming frames), and c = 3.6 km/s (the velocity of the forefront of the longitudinal unloading wave). During the time $2\Delta t$, the front will cover the distance of about $2L_0$, i.e., the end will then interact with the reflected compression wave and will change its velocity. The displacement during this time being known, we obtain v_0 = 86 m/s. Analogously we measure this velocity after arrival of the reflected wave to the free end: v_1 = 36.4 m/s. Then it remains constant for a long time (during the time sufficient for several reflections to take place). Instead of the wave motion, there appears motion of the fiber as a rigid whole in the longitudinal direction because of the transformation of the energy of longitudinal waves into that of the flexural waves owing to dynamic instability. We would like to remind that in the ideal case the wave intensities are identical and the equality $v_1 = -v_0$ holds. However, wave reflection at a clamp is not ideal and the aforementioned wave energy transformation takes place. The velocities of flexural waves are determined using such a geometrical method.

Using the elementary theory of longitudinal waves in elastic thin rods, a theoretical value of the mass velocity beyond the front of an incident wave is determined with the equation $v_E = \sigma/\rho c$ = 48.2 m/s. The measured velocity v_0 turned out to be higher by the magnitude which exceeded a statistical spread. However, if we accept the hypothesis that the dynamic load is applied nonlinearly along the curve that is downwardly convex, this discrepancy can be explained. When the front of the unloading wave is shock-free, a Riemann wave with an extending front starts propagating rather than a step. Such unloading is schematically shown in Fig. 10, where e_E and e_n are the deformations according to the laws of linear and nonlinear unloading. The velocity c corresponds to the slope of the tangent to the unloading curve at the point σ, e. It is maximal in case of initial perturbations, since all subsequent perturbations propagate with velocities determined by smaller slopes of tangents to the unloading curve. It was found that, in the case of relatively small initial deformation ($e \le 5\%$), the equality $v_E = v_0$ holds only approximately, i.e., the unloading is close to linear. It is expedient to note that, in the case of linear unloading, the wave front in a real rod is smeared, but its width will be sufficiently small in the considered cases as compared to the characteristic length of the fiber that makes it possible to simulate the wave shape with a step function.

Thus, the proposed complex method, the wave amplitude excluded, makes it possible to estimate the degree of nonlinearity of the dynamic stress-strain diagrams.

Measurement of Unloading Wave Characteristics in Flat Polymer Films

A complex method of determining characteristics of wave processes tested during investigations of fibers was modified as applied to the polymer film specimens. A polystyrene film for HP Lomond 0710425 laser printers with the thickness h = 142 μm and GOST R 51121-97, San Pin 24707-93, art. SV-104 polypropylene films (paper files) (Russia) with h = 32 μm were used. The experiments were carried out at room temperature. The film was cut into stripes with the width w = 5–30 mm and the length L = 20–30 cm and fixed in the clamps of a mobile cross-arm with a slight extension. Then one or two symmetric cuts were

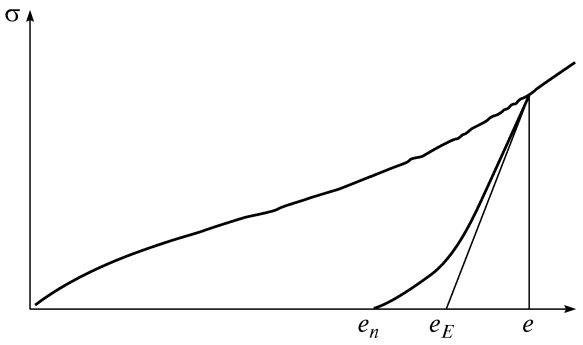

Fig. 10. Schematic of dynamic fiber unloading.

made in the analyzed specimen with a razor perpendicular to the free sides. The mobile clamp was manually set in motion with a jerk, whereas the other one was fixed. The loading rate of 1–5 m/s was not fixed, since the measured quantities weakly depended on it. When a soft load (the force F with the critical value) was reached, an accelerated motion of a crack started from the cut end to the opposite side of the cut and, after disintegration, an unloading wave began propagating from the formed free end. Fast processes of rupture and wave formation yielded variations in the electric field in the vicinity of the specimen, and it was reflected on the oscillograms, as was the case with fibers. The velocity of the generated unloading wave was measured according to the scheme in Fig. 5.

A typical oscillogram is shown in Fig. 11. A sharp bend in the shape of the left signal from the channel C_1 corresponds to the moment of disintegration, a slow signal increase proceeding to it is related to propagation of the crack in the analyzed specimen, and a subsequent fast increase is attributed to the unloading wave. The process of rupture was not recorded on a corresponding oscillogram, owing to the remoteness of another sensor from the place of fracture.

Some Measurement Results

According to our measurements, the density of the HP film is $\rho = 1334$ kg/m^3. In the first run of experiments, it was cut into stripes 2.5–2.8 cm wide. The initial cut d was half of the stripe width. Owing to orthotropy, the average velocity c in the film cut along and across the extension direction during fabrication was different and came to 2.1 and 1.94 km/s, respectively, the dispersion being negligible. Wave deformations were small, and it can be considered that it is appropriate to use the linear theory of viscous elasticity with the instant elasticity moduli $E = \rho c^2$ related to the observed processes for data processing. According to the formula, they came to $E = 5.88$ and 5.02 GPa, respectively.

For the sake of comparison, other experiments with the HP film with longitudinal cutting of stripes with a width smaller than 5 mm in which limit stresses were substantially larger were carried out. The average wave velocities slightly decreases: $c = 1.91$ km/s.

Analogous experiments made it possible to measure the velocity of the unloading wave in the stripes from a thinner polypropylene film ($\rho = 870$ kg/m^3) cut along and across its extension direction: $c = 2.3$–2.7 and 1.8–2.0 km/s. Correspondingly, the elasticity moduli at instant elastic unloading were within the ranges of 4.6–6.1 and 3.5–4.6 GPa. The difficulties of operating with these specimens were mainly attributed to the fact that an electric signal from the traveling wave was weak, and very often it was impossible to record the diversity of the signals t_0.

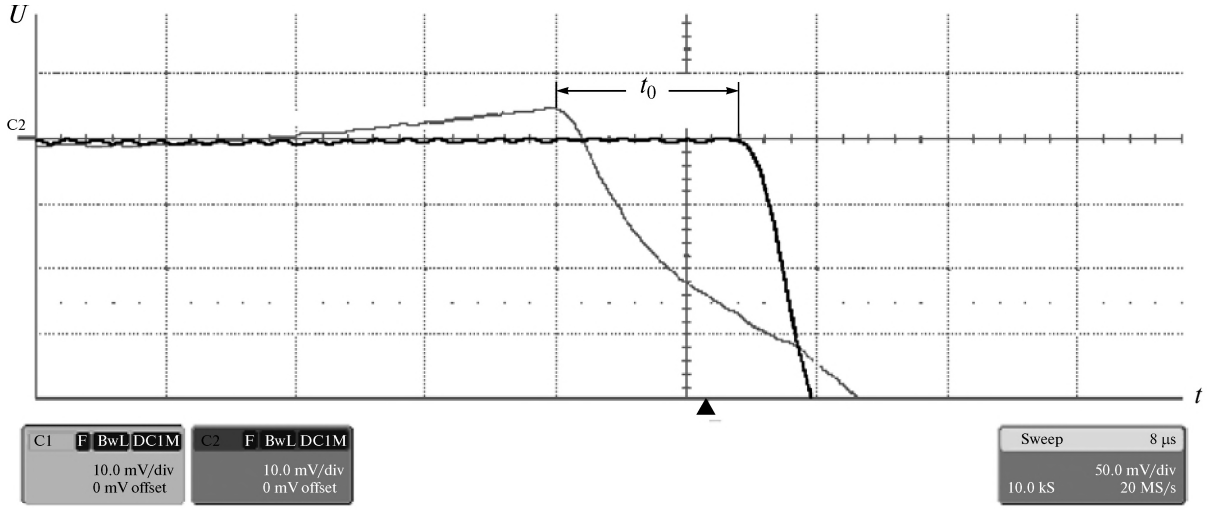

Fig. 11. An electrical signal from the crack motion and wave propagation in an HP film stripe.

Table 3. Mass, wave velocities, stress, and deformation jumps on the front and instant elasticity moduli for the HP film

v, m/s	l, cm	t_0, μs	c, km/s	Δe, %	σ, MPa	E, GPa
28.8	19	90	2.1	1.37	81	6.0
28.0	21	110	1.9	1.47	71	4.8
27.0	18.5	100	1.85	1.46	67	4.6

A possibility to simultaneously measure the wave and mass velocities of an unloading wave in a film stripe and, based on these data, to determine the stress and strain jumps on the wave front was demonstrated. Two symmetric cuts 1.5–2 mm long were made in a 1-cm-wide stripe along the direction of the film extension, perpendicular to the free surfaces to minimize the effect of the moment forming during stripe rupture. The region near the cut was blackened with a fiber-tip pen. During the experiments one of the antennas was positioned at the place of a cut, whereas the other was fixed near the remote clamp. As before, a force was applied to the mobile clamp as a jerk, the stripe was damaged, an unloading wave was generated, and the wave velocity was calculated based on the diversity of the signal recorded by the sensors and the base. In parallel, the vicinity of the place of the damage was filmed with a video camera at a rate of 27 000 frames per second and the frames of the motion of the formed free end were processed with a PC to calculate the mass velocity beyond the unloading wave front.

As has already been noted, the process of damage was not recorded by the second sensor and a sharp increase in the signal pointed to the arrival of the wave front with large deformation gradients. Thus, in the first approximation, the structure of the wave front can be ignored and its real shape can be substituted by a shock assuming that the wave is steplike. Making use of the laws of conservation at a shock and correlations of the linear elasticity theory, the jumps of deformation Δe and stress σ on the wave front, as well as the instant elasticity modulus E corresponding to unloading, were determined based on the wave and mass velocities c and v using Eq. (3).

The results of three experiments are listed in Table 3. The wave velocities slightly differ from the earlier-measured ones despite different experimental conditions and, as a result, different ultimate effective stresses and wave amplitudes.

Identical experiments were carried out for thin film stripes. For the stripes cut in the extension direction the following results were obtained during three experiments: $c = 2.4$, 2.3, and 2.0 km/s; $v = 19.5$, 27, and 27 m/s; $\sigma = 40.7$, 54, and 50 MPa; $e = 0.81$, 1.17, and 1.35%; and $E = 5.0$, 4.6, and 3.5 GPa. The mass velocities turned out to be in good agreement with each other. The wave velocities varies with a 10% error, since owing to the weakness of the electric signal, its beginning is not clearly shown in the oscillogram. It yielded a spread in the values of e, σ, and E, which, however, is typical during dynamic tests of any materials, especially polymers.

Let us now give the results of measurements for the thin film stripes cut perpendicular to the extension direction in two successful experiments: $c = 2$ and 2.3 km/s; $v = 17.6$ and 20.3 m/s; $\sigma = 32$ and 42 MPa, $e = 0.88$ and 0.88%, and $E = 3.6$ and 4.8 GPa. The measured parameters of the unloading wave turned out to be close to the analog parameters of the stripes cut in another direction: the anisotropy did not substantially affect the results.

CONCLUSIONS

The fundamental studies using recording of an electric signal are aimed at development and improvement of the means for inspecting the phenomena of rupture, oscillations, and propagation of waves in materials and structural elements at a micro-nano level. A number of methods of experimental investigation of oscillations and waves in micromechanics have been developed, and unique experimental setup for recording electric signals with an aim to identify dynamic processes in thin fibers and films have been designed. The methods, based on electromagnetic radiation recording, are characterized by the following advantages. They are noncontact, i.e., do not require positioning of auxiliary elements on a specimen, contrary to the traditional methods, which is of vital importance for micron-size objects; allow one to perform measurements under conditions of high and low temperatures and/or in the presence of an aggressive environment; do not require complex and expensive equipment; and the specimens are prepared using a standard technique. A possibility of studying oscillations of micron-diameter fibers, as well as regularities of propagation of longitudinal and transverse waves in polymer fibers and films, is demonstrated. A new complex method of measuring wave and mass velocities in thin polymer specimens during simultaneous application of the EMR-effect and high-speed photography that makes it possible to completely determine the parameters of longitudinal and transverse waves is proposed. The dynamic parameters of fiber and film materials are estimated depending on the intensity of loading and the scale effect. Note that the problems of material parameter reconstruction based on variations in the parameters of oscillations and waves often attract the attention of researchers [13, 14].

ACKNOWLEDGMENTS

The author is grateful to Head of Laboratory of Reinforced Plastics with the Institute of Chemical Physics of the Russian Academy of Sciences A.M. Kuperman and the specialists of this laboratory

for producing glass fiber specimens, as well as to Yu.K. Bivin, E.A. Devyatkin, and A.A. Sirotin for development and creation of new experimental setups and repeated discussion of the results. The experiments were performed by I.M. Smirnov and A.V. Tyanin, and the author appreciates their assistance.

The study was supported by OEMMPU program no. 12 and the Russian Foundation for Basic Research (project no. 07-01-12031).

REFERENCES

1. B. Tsoĭ, É. M. Kartashov, and V. V. Shevelev, *Strength and Fracture of Polymer Films and Fibers* (Khimiya, Moscow, 1999) [in Russian].
2. I. I. Perepechko, *Acoustical Methods of Polymer Study* (Khimiya, Moscow, 1973) [in Russian].
3. *Fiber Fracture*, Ed. by M. Elices and J. Llorca (Elsevier, Amsterdam, 2002).
4. Yu. K. Bivin, V. V. Viktorov, Yu. V. Kulinich, and A. S. Chursin, Izv. AN SSSR, Mekh. Tverd. Tela, No. 1, 183 (1982).
5. G. A. Lushcheĭkin, *Polymer Electrets* (Khimiya, Moscow, 1984) [in Russian].
6. I. V. Simonov and I. M. Smirnov, Preprint No. 836 (IPMekh RAN, Moscow, 2005).
7. I. V. Simonov, A. A. Sirotin, I. M. Smirnov, and A. V. Tyanin, Pis'ma Zh. Tekh. Fiz. **33** (14), 19 (2007) [Tech. Phys. Lett. **14**, 594 (2007)].
8. I. V. Simonov and A. V. Tyanin, Prikl. Mekh. Tekh. Fiz. **50**, 219 (2009).
9. Yu. N. Rabotnov, *Mechanics of Deformed Solid State* (Nauka, Moscow, 1979) [in Russian].
10. I. V. Simonov and I. M. Smirnov, Dokl. Akad. Nauk **422**, 185 (2008) [Dokl. Phys. **53**, 500 (2008)].
11. I. V. Simonov and I. M. Smirnov, Preprint No. 880 (IPMekh RAN, Moscow, 2008).
12. I. V. Simonov, Dokl. Akad. Nauk **428**, 330 (2009) [Dokl. Phys. **54**, 440 (2009)].
13. A. N. Bekhterev, Akust. Zh. **54**, 26 (2008) [Acoust. Phys. **54**, 20 (2008)].
14. O. V. Bocharova and A. O. Vatul'yan, Akust. Zh. **55**, 275 (2009) [Acoust. Phys. **55**, 281 (2009)].